# On the Implementation of Embedded Communication over Reflectometry-oriented Hardware for Distributed Diagnosis in Complex Wiring Networks

Esteban Cabanillas, Moussa Kafal, Wafa Ben Hassen

# On the Implementation of Embedded Communication over Reflectometry-oriented Hardware for Distributed Diagnosis in Complex Wiring Networks

Esteban CABANILLAS, Moussa KAFAL, *Member, IEEE*, Wafa BEN-HASSEN
CEA, LIST, Laboratoire de Fiabilisation et d'Intégration des Capteurs
Nano-Innov, Bât. 862-PC172, 91191 Gif-sur-Yvette Cedex, France

***Abstract*—In this paper, the first electronic device capable of performing simultaneous Orthogonal Multi-Tone Time Domain Reflectometry (OMTDR) measurements with data fusion is presented. This is possible by executing reliable communication among several OMTDR-based systems. In fact, the main challenge of any developed system is to achieve a zero bit error rate communication with a typical reflectometry hardware without considering complex clock recovery systems and synchronization blocks. To achieve that, the proposed system must to be able to find the minimum interference sampling time in a short delay in order to avoid synchronous issues. This is achieved by performing a novel fast time distributed oversampling technique. Such technique consists of sampling the Analog-to-Digital Converter (ADC) and the Digital-to-Analog Converter (DAC) with a frequency offset, achieving $\Omega$ order oversampling in $\Omega + 1$ OMTDR signal cycles. The developed demonstrator is capable of ensuring cable diagnosis and reliable communication between several devices connected with aeronautical cables.**

## I. Introduction

Electrical wiring systems are highly likely exposed to severe external and internal conditions (i.e. heat, vibration, manufacturing defects, etc.) leading to cable aging and degradation. Thus, an embedded health monitoring system for continuous cable diagnosis becomes crucial [1], [2]. Recently, on-line wire diagnosis using reflectometry has been under intensive investigation, aiming at detecting faults on wiring networks while the target system is in normal operation [3], [4].

Significantly, Orthogonal Multi-tone Time Domain Reflectometry (OMTDR) using ultra-wide band test signals constructed using the Orthogonal Frequency Division Multiplexing (OFDM) principle succeeded in this mission [5]. The idea is to divide the bandwidth into multiple sub-bands using orthogonal and then overlapped sub-carriers which permits a total spectrum control. As a matter of fact, Multi-Carrier Reflectometry (MCR) and its variant OMTDR have shown promising potential in detecting and locating faults in an online live manner [2], [5], [6].

However, as any reflectometry based technique, they suffered from signal loss related to wiring system attenuation. Indeed, the attenuation of the signal is mainly caused by the cable's resistance: it reduces the amplitude of the signal during the propagation and therefore limits the performance of the diagnosis. This phenomenon is mainly encountered on long cables and becomes more critical in complex wiring networks due to the presence of splices, connectors, etc. In such networks, a further level of complexity is added which is demonstrated by ambiguity problems attached to multiple paths phenomenon which in turn complicates the analysis of the reflectometry response and leads to false alarms [1].

To cope with the aforementioned problems, a distributed diagnosis strategy is proposed. Several testing systems can be placed at strategic points of the network under test (NUT) thus enabling reflectometry measurements according to their perspective of the NUT. Besides, it is possible to activate each testing system alternately. However, it shall be better to activate all testing systems simultaneously to ensure that the same NUT is processed for each one of them, especially in embedded systems. Unfortunately, interference noise problem related to the simultaneous injection of reflecometry signals of different testing systems would appear.

Within this context, several methods have been proposed in the literature to cope with signal interference issues [7]–[9]. In [10], customized testing signals using specific sequences (i.e. M-Sequence) with low cross-correlation amplitudes were considered. In fact, the method shares the same concept used in Sequence Time Domain Reflectometry (STDR) [3]. Notwithstanding the methods' low complexity, they require a synchronization step among sensors and the sequences should be regenerated once a new network is tested. Moreover, the choice of the testing signals (i.e. signal spectra) can be limited by the application constraints.

As solution, a selective average based method has been introduced in [11] which exploits the averaging operation using weighting coefficients at the emission and reception sides. It may be extended to larger variants of reflectometry (STDR, MCR, OMTDR, etc.). The selective averaging method makes it possible to obtain negligible interference noise levels by using the Walsh-Hadamard or Rademacher sequences according to the synchronous or asynchronous case. However, the selective averaging method is very complex and the considered hypotheses (i.e. the network stationarity during the averaging process) are difficult to maintain in practice.

In conventional methods [10], [11], the testing system which is often referred to as *reflectometer* has the exclusivity to perform its own diagnosis and make the decision on the location of the fault independently from other reflectometers. Nevertheless, since the diagnosis function is distributed and integrated at different points of the NUT, communication is essential between different reflectometers to ensure information aggregating to a central one (i.e. master sensor). Particularly, this permits to decrease blind zones, increase the network coverage and facilitate decision making [12].

In this paper, the first electronic device capable of performing simultaneous OMTDR measurements with data fusion by executing reliable communication among several OMTDR-based systems will be introduces. To the best of our knowledge, the implementation of communication on a reflectometry

measurement-oriented device has never been done with existing cable health monitoring systems. The main challenge of the developed system is to achieve zero bit error rate communication with a typical reflectometry hardware which does not consider complex clock recovery systems and synchronization blocks. To achieve that, the proposed system must to be able to find the minimum interference sampling time in a short delay in order to avoid synchronous issues. This is achieved by performing a novel fast time distributed oversampling technique. The paper will be organized as follow: Section II introduces the OMTDR devices and their synchronous issues forbidding reliable data communication. This is followed by presenting a novel fake-oversampling technique allowing synchronization between reflectometry boards in sec. III. In order to validate the feasibility of the proposed approach, section IV performs implementation of an embedded communication system and some hardware tests. The last section concludes the paper.

## II. Distributed OMTDR traditional hardware

A simplified model of an OMTDR system performing wire diagnosis is presented in Fig. 1. The arbitrary OMTDR block generates a multi-carrier digital signal $s_n$ composed of $N$ sub-carriers based on the OFDM modulation technique. As exposed in [5], the sub-carriers must be distributed by respecting the hermitian symmetry concept thus producing a real signal $s_n$. The OFDM technique starts by setting the phase of the first $N/2$ sub-carriers by applying an M-PSK mapping. Each sub-carrier $S_k$ is defined as:

$$|S_k| = 1 \ \forall \ f_n \quad \text{and} \quad \phi(k) = \phi_n = i\frac{2\pi}{M} \tag{1}$$

where $M$ is the PSK order (4 for Q-PSK, 8 for 8-PSK, etc.) while $i$ is a parameter taking any value between 0 and $M-1$. The hermitian symmetry is obtained by defining the remaining sub-carriers as:

$$S_{N-k} = S_k^* \tag{2}$$

After that, an inverse fast-Fourier transform (IFFT) is employed to generate the time domain version of $s_n$ from the modulated sub-carriers after-which a DAC generates $s(t)$, the analog time domain signal. $s(t)$ is the OMTDR generated testing signal that is injected to the coupler linking the DAC with the cable under test (CUT) and the ADC. The injected signal $s(t)$ travels over the CUT and reflects back once an impedance mismatch (IMis) is met. In this case, the reflected signal $r(t)$ is sampled by the ADC to produce $r_n$, the reflected digital signal. A correlator block computes the cross-correlation function $\Gamma_{rs_n}$ between the injected signal $s_n$ and the reflected signal $r_n$. In effect, $\Gamma_{rs_n}$ is plotted in the form of a reflectogram whose analysis and post-processing allows locating the impedance mismatches embedded in the NUT.

On the other hand, ensuring a reliable detection and classification of IMis requires a good signal-to-noise ratio (SNR) of the received signal $r_n$. However, cables can be strongly dispersive especially when tested on a high frequency basis. Regrettably, it is the case of the OMTDR testing signals which are generated at a high frequency bandwidth. For instance, the power of a reflected signal caused by an IMis located at the end of a CUT can be below the noise level. In this case, the IMis reflected echo is undetectable for the reflectometry system.

The implementation of a distributed reflectometry system avoids blind zones in the CUT/NUT. In fact, this technique consists on placing reflectometry testing devices on multiple cable endings. Each device transmits its own reflectogram to a master device. The master performs a global analysis of the data received from each device connected to the network thus producing a higher level of precision for the CUT/NUT diagnosis. Notably, the number of reflectometry devices required for integration in a NUT depends on the length of cables and the network's topology complexity. It is noteworthy that performing reliable communication of processed data to a master device is a critical issue.

Standard reflectometry hardware can handle data communication since it integrates a transceiver composed of a transmission block (DAC) and a reception block (ADC). Fig. 2 illustrates two reflectometry devices with bounded couplers. In this implementation, the arbitrary OMTDR block of fig. 1 is replaced by an OMTDR modulator. At the reception side, the ADC digital output is now also connected to an OMTDR demodulator, implemented in parallel with the correlator computing the reflectogram. For such a system, each reflectometry device is capable of computing its own reflectogram $\Gamma_{rs_n}$. The reflectogram produced data can be processed by the OMTDR modulator in order to be sent to a distant reflectometry device. In fig. 2, message $b1$ represents the message containing the reflectogram computed by the left side device. This OMTDR message is then transmitted to the ADC of the right side device. The OMTDR block demodulator extracts the left-sided reflectogram from the acquired signal. In the same manner, the right-sided device can later compute its own reflectogram. Consequently, after this process, a good diagnosis of the health of the CUT/NUT bounding the devices can be achieved since blind zones in the reflectogram are avoided with the combination of the acquired (from correlator) and received (from OMTDR demodulator) reflectograms.

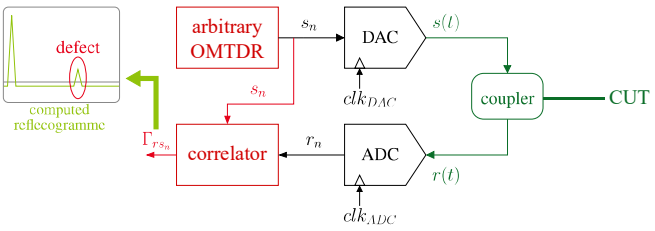


Fig. 1. Schematic diagram of a standard OMTDR reflectometry based wire diagnosis system performing correlation between the injected signal $s(t)$ and the received signal $r(t)$ to detect faults.

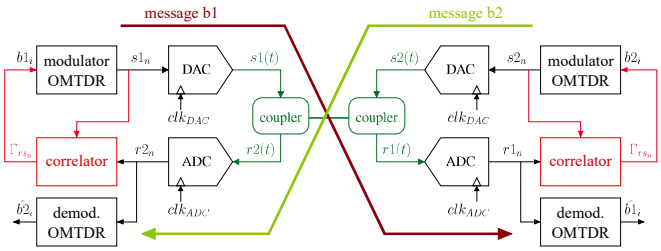


Fig. 2. Two reflectometry devices are connected to the same NUT in order to effectuate OMTDR communication based reflectometry.

Reflectometry devices are designed to generate and acquire synchronous signals. Accordingly, the digital reflectometry core provides synchronous clocks to drive the DAC and the ADC. This synchronous scenario is no longer valid when two or more reflectometry devices perform communication. Notably, any frequency dispersion in crystals used to generate clocks in each hardware could yield synchronization related issues thus prohibiting a free-error bit communication.

Synchronization issues over OMTDR communication are demonstrated on Fig. 3. It illustrates two versions of the received signal $r(t)$ inside a time interval equal to $3T_s$, with $T_s$ being the ADC sampling time. In red, the received signal has unlimited passband (ideal DAC output); in blue, the received signal is defined in the Nyquist band. Since the blue signal is the result of a filtering process, an optimal sampling instant with minimal interference should be found inside the sampling time period $T_s$. This sampling instant is illustrated with two points over the received signal where $A0$ is a point that happens at $NT_s$ while point $A1$ at time $NT_s + \phi_{opt}$. It is shown that acquiring the signal with a phase $\phi_{opt}$ shall be optimal in terms of signal integrity. On the contrary, if the reception is done at time $NT_s$, the interference shall be strong enough to forbid the transmission.

The effect of the sampling instant over the integrity of the received data is illustrated on Fig. 4. Both constellations are obtained from a free noise transmission implementing 8-PSK digital modulation on the OMTDR sub-carriers. The left side figure shows the received constellation when the sampling is done at time $NT_s + \phi_{opt}$ (point $A1$) while the right sided one is done at time $NT_s$ (point $A0$). Notably, free interference received data is obtained with the optimal sampling instant of point A1. On the other hand, sampling at a bad instant, i.e to say point $A0$, induces high interference in the received data. Markedly, such an interference when combined with some channel noise can induce a high bit error rate thus greatly degrading the reliability of data transmission and decline the accuracy of NUT diagnosis.

As synchronization issues are not considered to perform

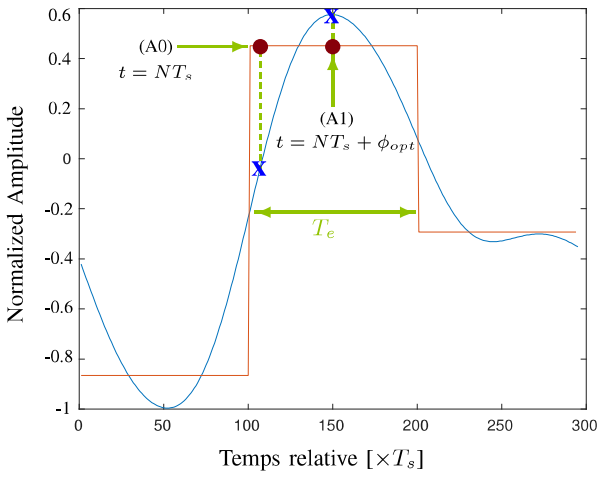


Fig. 3. OMTDR signals into a $3T_s$ interval. The red signal is transmitted with infinite wide-band while the blue signal wide-band is limited to nyquist frequency ($T_s/2$). The acquisition of both signal is done at two different instant, point A0 and A1.

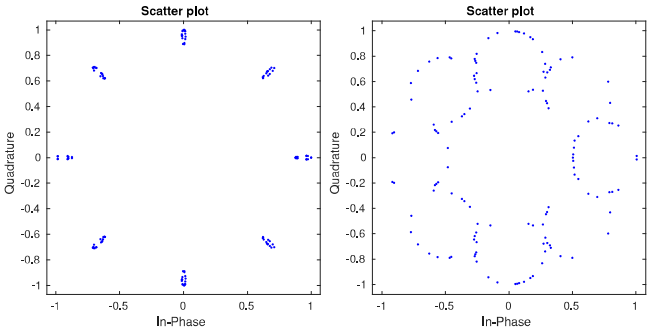


Fig. 4. Received constellation carried by an OMTDR signal whose sub-carriers are 8-PSK digital modulated. For the left side constellation, the sampling instant is that of point A1 (Fig. 3). The right side constellation is acquired by point A0.

reflectometry at a single point, no re-synchronization block or clock recovery block are implemented on typical reflectometry hardware. The absence of such a block is a real obstacle for performing a reliable communication through reflectometry devices. Nevertheless, smart acquisition techniques can help to work near the optimal sampling phase $\phi_{opt}$, permitting the system to communicate without adding additional hardware to ordinary reflectometry boards.

## III. Fake-oversampling method for re-synchronization

The previous section has shown that an optimal acquisition is possible by sampling the acquired data at an accurate time, referred to $\phi_{opt}$. As a matter of fact, determining that optimal point is normally done by synchronization blocks. On the other hand, $\phi_{opt}$ could be marked by oversampling the acquired signal, i.e to say the ADC sampling frequency shall be $\Omega$ times bigger than DAC's one, with $\Omega$ being the oversampling ratio. Unfortunately, this will physically limit the ADC accuracy and skyrocket its cost leading to a non-practical system implementation from a commercial marketing aspect. This section will present a promising method for drastically growing the capacities of the ordinary implemented ADC, by performing a fake-oversampling technique.

Taking into account that the emitted signal $s_n$ is periodic, it becomes sufficient to consider multiple repetitions of this signal over a longer amount of time. This is followed by sub-sampling the received signal to reconstruct a new signal $r_n$ which will be an equivalent of an oversampled reconstructed signal.

This approach might recall Verniers method of distance measurement but applied to a periodic time measurement with a finite subdivision. Thus, the system is constructed so that the ADC sampling period ($T_{\text{ADC}}$) is spaced at a constant fraction of the fixed DAC sampling period ($T_{\text{DAC}}$).

With $\Omega$ being the oversampling factor to be achieved, it is sufficient to increase $T_{\text{ADC}}$ such that

$$T_{\text{ADC}} = T_{\text{DAC}} \cdot \frac{\Omega + 1}{\Omega} \tag{3}$$

The received signal is then acquired at every $T_{\text{ADC}}$ step so

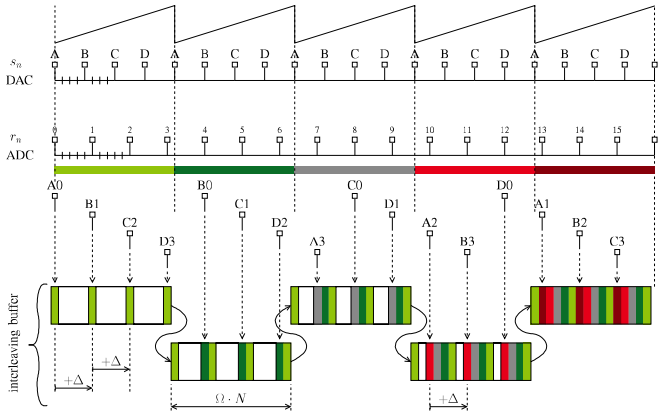


Fig. 5. Representation of a simplified version of the oversampling method using a constant frequency offset between the DAC and the ADC. The injected signal is composed of four samples (A, B, C and D). The oversampling factor $\Omega = 4$ and $f_{ADC} = 4/5 \cdot f_{DAC}$.

that each sample is interleaved

$$r(t + T_{\text{ADC}}) \mapsto r_{n+1} \mapsto r'_{(n+\Delta) \bmod [N \cdot \Omega]} \tag{4}$$

where $N$ is the number of points of the transmitted OMTDR signal.

The register structure to acquire the received oversampled signal is a simple reordering buffer with a constant interleaving scheme. The write memory address is calculated with an adder of $\Delta$ modulo $N \cdot \Omega$ and the read memory address is simply incremental.

Fig. 5 represents a simplified version of the oversampling method described in this section using a constant frequency offset between the DAC and the ADC, where a periodic signal $x(t)$ is sent through the CUT with four samples (A, B, C and D). The oversampling factor is hereby $\Omega = 4$ and $f_{\text{ADC}} = 4/5 \cdot f_{\text{DAC}}$. Hence, the acquired oversampled signal is composed of 4 sets of samples, where each set is obtained from a different sampling instant. Notably, the presented oversampling process does not require any high-performance DAC or ADC devices. As a result, less complex and lower cost systems are achieved.

Once the oversampling is accomplished, the acquisition block must analyze each set of samples in order to find the optimal one. This is done by computing the average value of each set and then taking that of the maximal average value. For instance, Fig. 6 shows the average value of each set of acquisitions ($\Omega = 16$) of the band-limited OMTDR signal

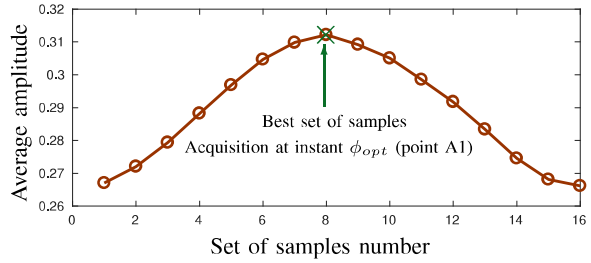


Fig. 6. Average amplitude of each received set of samples of an oversampled OMTDR signal with passband equals to $f_{Nyquist}$. The oversampling factor is $\Omega = 16$.

shown in Fig. 3. Indeed, the highest average value is found at the instant described by point $A1$. That same instant leads to a minimal interference of the received constellation.

In what follows, we will describe the implementation of the transceiver integrating the fake re-synchronization technique with an original protocol used to carry out reliable communication.

## IV. On the Implementation of an OMTDR Communication System

### A. OMTDR communication protocol

The method used to communicate data between reflectometry devices is based on a master-slave protocol. That protocol is described by the sequence of Fig. 7. The protocol starts when the master asks one of the slaves to compute a reflectogram and then transmits it back to the master. The request message is composed of several non-zero sub-carriers. Consequently, since an OMTDR signal is composed of $N$ sub-carriers, each slave shall answer to a predefined set of $k$ sub-carriers, with the rest of sub-carriers forced to zero.

Each slave receives the master request but only one of them is programmed to answer for this request. The selected slave performs the OMTDR reflecometry after the request. The signal used to perform reflectometry is an arbitrary OMTDR signal, which is a-priori known by the master. The same signal is also used by the master to compute the equalizer. Accordingly, during the period when the slave injects the OMTDR signal over the NUT, the master acquires that data to determine the attenuation and the phase shifting of each received sub-carrier. That information is used to compute the equalizer that allows the receiver to compensate for the impairments induced by the channel (NUT) over each sub-carrier.

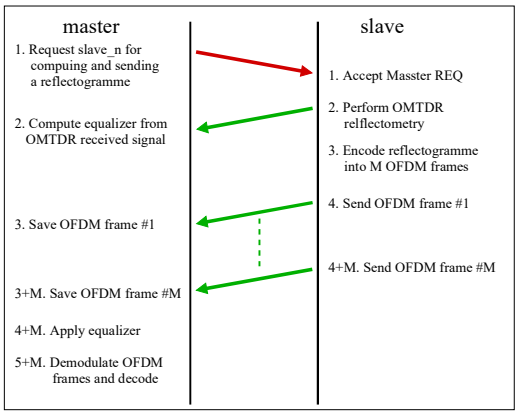


Fig. 7. Communication protocol used to transfer data between an OMTDR master and an OMTDR slave.

The reflectogram computed by the slave must be send to the master in order to perform distributed reflectometry diagnosis. To achieve that, the whole reflectogram composed of $N$ points must be decomposed on $N \cdot Q$ bits, with $Q$ being the quantification of each point of the reflectogram. These bits are grouped on $M$ frames that are digitally treated by the transmitter presented in Fig. 8. Notably, the digital process is inspired from the digital architecture used by DVB-S2 standard

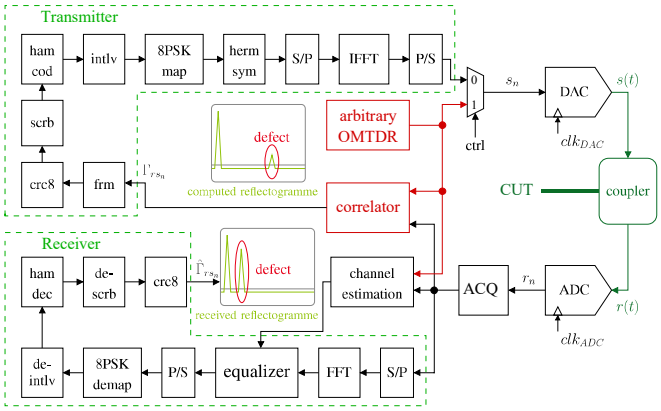


Fig. 8. A schematic diagram of the OMTDR transceiver performing wire diagnosis from correlation based reflectometry and OMTDR based data communication.

[13]. In fact, the Block form divides the $N \cdot Q$ bits of the whole reflectogram into $M$ groups of $\Theta$ bits. The values of $\Theta$ and $M$ are defined by the capacity of the $N$ points OMTDR signal to carry binary information $N_{b_{omtdr}}$. For a standard 128-points OMTDR signal ($N$=128) and an 8-PSK mapping, the OMTDR capacity is given as follows:

$$N_{b_{omtdr}} = (N/2 - 2) \cdot 3 = 186. \quad (5)$$

Where $N/2-2$ represents the number of useful carriers since a Hermitian symmetry is necessary to generate a real valued signal. The efficient number of bits ($\Theta$) of each OMTDR signal is then limited by the Hamming code rate, which adds redundancy bits to the information bits. The implemented code rate is $11/15$, i.e. 4 redundancy bits are added to 11 information bits in order to perform binary error correction. Then, $\Theta$ can be computed as:

$$\Theta = 11 \cdot ceil(N_{b_{omtdr}}/15) = 143 \quad (6)$$

Taking the quantification of each reflectogram point $Q = 10$, the number of frames needed to transmit the whole reflectogram is defined by:

$$M = ceil((N \cdot Q)/\Theta) = 9 \quad (7)$$

Once the $M$ groups of bits are defined, they are sent one after the other to the binary block-chain. The first binary function is a cyclic redundancy check of order 8 (CRC8), which provides a verification utility for message integrity test. After that, the bits are scrambled based on [14] in order to give a uniform power to the sent data. The main Hamming encoding with a rate $11/15$ is applied at the end of the chain [15]. After that, a bit interleaving procedure is performed to enhance the binary correction capacity of the system [16]. The remaining part of the transmitter is composed of classical OMTDR blocks. An 8-PSK mapping block defines the phase of each sub-carrier. Hermitian symmetry is then applied in order to get a real time-domain signal. The sub-carriers are presented in a parallel mode (S/P block) to the IFFT block, whose output is the time-domain OMTDR signal. That signal is serialized (P/S) and converted to the analog domain by a DAC.

The transmitter will send $M$ different OMTDR frames as shown in Fig. 7. Each frame is injected during several cycles, depending on the oversampling factor $\Omega$ implemented at the receiver side. As explained on Fig. 5, the receiver need $\Omega + 1$ OMTDR signal cycles to perform $\Omega$-order oversampling. The receiver block ACQ chooses the best set of samples from $\Omega$ set of samples. This is done by following the method of the average value, Fig. 6. After choosing the best acquisition, each frame is transformed to the frequency domain by applying a FFT function. The frequency domain signal is equalized by compensating the phase-shift and the attenuation of each sub-carrier. Such phases and attenuations have been computed at the beginning of the protocol. The received bits are extracted from the set of sub-carriers by 8-PSK de-mapping. After that, bit de-interleaving is applied which is followed by a hamming code error correction and a bit de-scrambling. Finally, a CRC8 block allows the receiver to decide whether the received set of bits contain binary errors or not.

### B. Hardware implementation

In order to test and validate the feasibility of the proposed embedded OMTDR communication approach, the OMTDR transceiver presented in Fig. 8 has been physically implemented on a reflectometry board. The board integrates a Xilinx ZYNQ 7010 FPGA driving a 10 bit ADC and a 10 bit DAC. The DAC sampling frequency is $F_{CLK_{DAC}} = 188.8$ MHz and the ADC's sampling frequency is $F_{CLK_{ADC}} = 177.7$ MHZ. The ratio between $F_{CLK_{DAC}}$ and $F_{CLK_{ADC}}$ allows the receiver to perform an oversampling rate $\Omega = 16$. Three boards have been connected to the same NUT which is configured with a "T" topology as shown in Fig. 9. The cable linking the boards is an aeronautical cable MLB24, widely used for CAN bus based communication.

The reflectograms obtained from the OMTDR MASTER block are presented on Fig. 10. The obtained reflectogram shows the master's computed reflectogram (blue line) and the reflectograms transmitted from OMTDR SLAVE1 (dotted red line) and OMTDR SLAVE2 (dashed green line). All reflectograms present a high value peak near 0 m. These peaks are induced by the mismatch between the board coupler output impedance and the cable impedance. The first peak after the coupler is found in the MASTER reflectogram, at 3 m from the coupler. This negative peak is generated by the impedance mismatch of the "T" junction. The same impedance mismatch is found at 13.5 m for the reflectogram transmitted by SLAVE1 and at 16.5 m for that of SLAVE2.

The interest of implementing communicating distributed reflectometry is highlighted by analyzing the master reflectogram after the negative peak at 3 m. Notably, two weak and spread peaks are present at 16.5 m and 19.5 m, both peaks are originated by the echoes coming from SLAVE1 and SLAVE2 couplers. Any additional echo induced by an impedance mismatch placed between the junction and SLAVE1

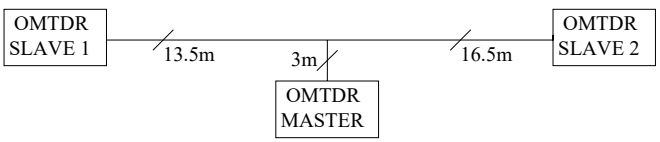


Fig. 9. Topology of the NUT implemented to test and validate the proposed OMTDR system.

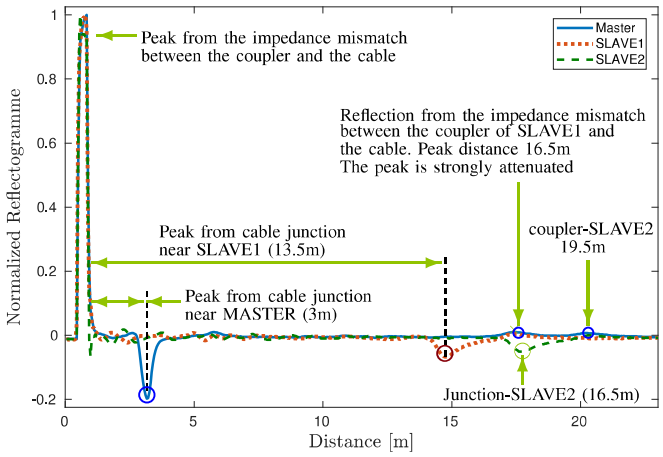


Fig. 10. Reflectograms obtained from the MASTER OMTDR. The blue line illustrates the MASTER produced reflectogram. Dotted red and dashed green lines represent the reflectograms transmitted to the master from SLAVE1 and SLAVE2 respectively.

or SLAVE2 shall be strongly attenuated, and impossible to be detected from the MASTER alone. The blind zone is no more real when the reflectogram is computed from another cable ending. In effect, the whole zone between SLAVE1 and the junction is well covered with the diagnosis done by SLAVE1. Notably, the negative peak placed at 13.5 m from the coupler of SLAVE1 has high amplitude and reduced spreading. The probability to detect any impedance mismatch in this zone is now strongly augmented. The same affirmation is also true for the branch connected to SLAVE2, permitting the system to perform reliable diagnoses over this part of the NUT.

## V. Conclusion

We have presented in this paper a novel approach based on the tents of standard OMTDR method and a fake-oversampling technique. In effect, reliable low bit-error-rate communication between different reflectometry devices implemented on the extremities of a tested network is ensured. Efficient diagnosis is preserved for networks lively operating with no interferences acquired neither between the reflectometry testing signals and the network's native signals nor between the testing signals themselves. Experimental results prove the potential adequacy of the proposed technique in precisely detecting and locating impedance mismatches in a network under test while canceling any localization ambiguity.

## References


[1] F. Auzanneau, "Wire troubleshooting and diagnosis: Review and perspectives," *Progress In Electromagnetics Research*, vol. 49, pp. 253–279, 2013.

[2] L. Incarbone, F. Auzanneau, W. B. Hassen, and Y. Bonhomme, "Embedded wire diagnosis sensor for intermittent fault location," in *SENSORS, 2014 IEEE*. IEEE, 2014, pp. 562–565.

[3] P. Smith, C. Furse and J. Gunther, "Analysis of spread spectrum time domain reflectometry for wire fault location," in IEEE Sensors Journal, vol. 5, no. 6, pp. 1469-1478, Dec. 2005.

[4] S. Naik, C. Furse and B. Farhang-Boroujeny, "Multicarrier reflectometry," in IEEE Sensors Journal, vol. 6, no. 3, pp. 812-818, June 2006.

[5] W. B. Hassen, F. Auzanneau, L. Incarbone, F. Pérès, and A. P. Tchangani, "On-line diagnosis using orthogonal multi-tone time domain reflectometry in a lossy cable," in *Proceedings of the 10th International Multi-Conference on Systems, Signals and Devices (SSD13)*, 2013, pp. 1–6.

[6] L. Incarbone, S. Evain, W. B. Hassen, F. Auzanneau, A. Dupret, Y. Bonhomme, F. Morel, R. Gabet, L. Solange, and A. Zanchetta, "Omtdr based integrated cable health monitoring system smartco: An embedded reflectometry system to ensure harness auto-test," in *Industrial Electronics and Applications (ICIEA), 2015 IEEE 10th Conference on*. IEEE, 2015, pp. 1761–1765.

[7] M. Kafal, J. Benoit, A. Cozza, and L. Pichon, "A statistical study of dort method for locating soft faults in complex wire networks," *IEEE Transactions on Magnetics*, vol. 54, no. 3, pp. 1–4, 2018.

[8] M. Kafal, J. Benoit, A. Cozza, and L. Pichon, "Soft fault diagnosis in wire networks using time reversal concept and subspace methods," *Proc. EEETEM*.

[9] M. Kafal, A. Cozza, and L. Pichon, "Locating faults with high resolution using single-frequency tr-music processing," *IEEE Transactions on Instrumentation and Measurement*, vol. 65, no. 10, pp. 2342–2348, 2016.

[10] N. Ravot, F. Auzanneau, Y. Bonhomme, M.O. Carrion and F. Bouillault, "Distributed reflectometry-based diagnosis for complex wired networks", Pin Proc. EMC Workshop: Safety, Reliability, Security Commun. Trans. Syst, 2007.

[11] A. Lelong, L. Sommervogel, N. Ravot and M. O. Carrion, "Distributed Reflectometry Method for Wire Fault Location Using Selective Average," in IEEE Sensors Journal, vol. 10, no. 2, pp. 300-310, Feb. 2010.

[12] W. Ben Hassen, F. Auzanneau, L. Incarbone, F. Pérès and A. Tchangani, "Distributed sensor fusion for wire fault location using sensor clustering strategy," International Journal of Distributed Sensor Networks, vol.11, no.4, 2015.

[13] Y. Murillo et al., "Multidisciplinary Learning through Implementation of the DVB-S2 Standard," in IEEE Communications Magazine, vol. 55, no. 5, pp. 124-130, May 2017.

[14] J. K. Lee, B. G. Yu and J. U. Kim, "Multicarrier Transmission Peak-to-Average Power Reduction Using Redundant Bit Scrambling," 2007 IEEE 66th Vehicular Technology Conference, Baltimore, MD, 2007, pp. 1274-1277.

[15] A. K. Singh, "Error detection and correction by hamming code," 2016 International Conference on Global Trends in Signal Processing, Information Computing and Communication (ICGTSPICC), Jalgaon, 2016, pp. 35-37.

[16] I. Kang, K. S. Ok, Y. Kim, J. H. Seo, H. M. Kim and H. N. Kim, "Design of a bit interleaver for the high-order constellation DVB-T2 system," 2014 IEEE International Symposium on Broadband Multimedia Systems and Broadcasting, Beijing, 2014, pp. 1-4.